

ON-LINE TEXTURE ANALYSIS FOR MAGNETIC PROPERTY CONTROL

H. J. BUNGE, H. J. KOPINECK and F. WAGNER

Inst. f. Metallkunde, Grosser Bruch 23, D-3392 Clansthal-Zellerfeld, Germany
Hoesch Stuhl AG, D-4600 Dortmund, Germany
Lab. de Metallurgie des Materiaux Polycrystallins, F-57045 Metz, France

Magnetic properties of hard and soft magnetic materials are strongly anisotropic, i.e. they depend on the crystal direction in which they are being considered. Technological materials are usually polycrystalline. Hence, their properties are orientation mean values of the properties of the crystallites with the texture of the material as the weight function. Inspection and control of magnetic properties of materials thus requires inspection and control of the materials texture which can be carried out off-line by taking samples from the finished material and investigating them in the laboratory. If, however, the texture of the material is to be controlled during the production process then a fast non-destructive on-line texture analyser is required the output signal of which can be used to control the production process.

KEY WORDS X-ray diffraction, energy dispersive method, transmission method, fixed angle texture analyzer, texture coefficients, pole figure window, magnetic anisotropy.

Figure 1 shows the principles of a fixed angle on-line texture analyzer, developed and applied for continuous r_m -determination in the cold rolling mill quality control of the Hoesch Stahl AG in Dortmund F.R.G. (see e.g. Kopineck, 1986; Kopineck and Otten, 1987; Kopineck and Bunge, 1989). The same principle can also be used for the determination of the direction dependence of many other anisotropic physical properties.

This paper gives the mathematical basis for the determination of the texture coefficients needed for on-line determination of magnetic properties. (For the relationship between these coefficients and the property values themselves see e.g. Bunge (this volume)).

The texture of a polycrystalline material is the orientation distribution of its crystallites

$$f(g) = \frac{dV/V}{dg}; \quad g = \{\varphi_1, \Phi, \varphi_2\} \quad (1)$$
$$dg = \frac{\sin \Phi}{8\pi^2} \cdot d\Phi \cdot d\varphi_1 \cdot d\varphi_2$$

Thereby g is the orientation of the crystal coordinate system K_B of an individual crystallite (e.g. the cubic axes) with respect to a sample coordinate system K_A , e.g. rolling, transverse, and normal direction of a sheet. The orientation g can be expressed by the Euler angles $\varphi_1, \Phi, \varphi_2$ and $f(g)$ describes the volume fraction of crystals which have an orientation g within the angular limits dg .

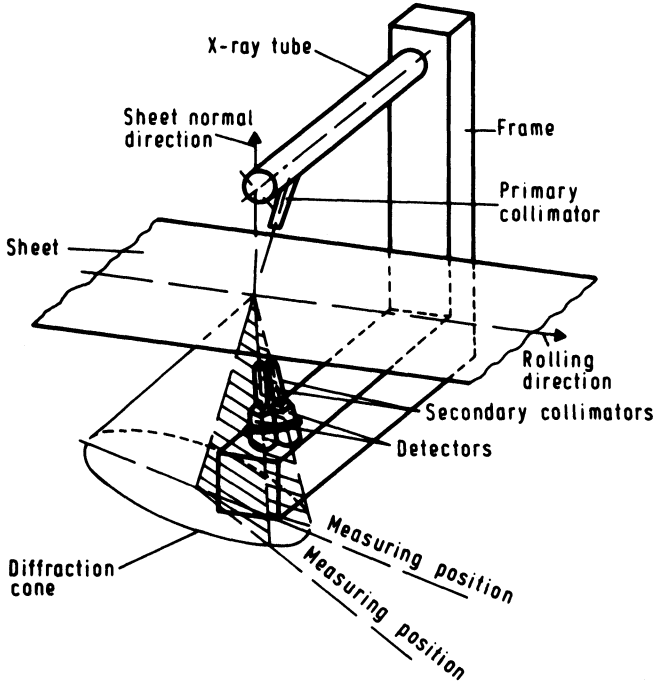


Figure 1 Principles of a fixed-angle, on-line texture analyser.

The texture function is needed in order to calculate texture mean values of direction depend physical properties. If $E(h)$ is the value of any physical property (e.g. the magnetization energy) in the crystal direction h then the mean value $\bar{E}(y)$ of this property in the sample direction y is given by

$$\bar{E}(y) = \oint E(h) \cdot A(h, y) dh \tag{2}$$

where $A(h, y)$ is the volume fraction of crystals, the crystal direction h of which is parallel to the sample direction y (see e.g. Bunge, 1982; Bunge, this volume). This function is an integral over the texture function $f(g)$

$$A(h, y) = \frac{1}{2\pi} \int_{h \parallel y} f(g) d\psi \tag{3}$$

The texture function $f(g)$ can be expressed in terms of a series expansion

$$f(g) = 1 + \sum_{\lambda=\lambda_0}^L \sum_{\mu=1}^{M(\lambda)} \sum_{\nu=1}^{N(\lambda)} C_{\lambda}^{\mu\nu} \cdot \hat{T}_{\lambda}^{\mu\nu}(g) \tag{4}$$

of generalized spherical harmonics $\hat{T}_{\lambda}^{\mu\nu}(g)$. The texture is then described by its coefficients $C_{\lambda}^{\mu\nu}$. For a complete description of the texture, the series must be extended up to relatively high L -values, e.g. up to $L = 22$. In the case of cubic crystals and textures in sheet materials (orthorhombic sample symmetry) the total

number of coefficients $C_{\lambda}^{\mu\nu}$ is then 185. This total number of coefficients is, however, not needed if only mean values of physical properties according to Eq. (2) are being considered. The direction dependence $E(h)$ of most of all physical properties is a low-order function of h (e.g. fourth or sixth order in the case of magnetic properties, see e.g. Bunge, 1982). Then only very few of the coefficients $C_{\lambda}^{\mu\nu}$ of Eq. (4) enter the mean value expression Eq. (2) (e.g. up to $L^0 = 4$ or $L^0 = 6$ in the case of magnetic properties). With cubic crystal symmetry and orthorhombic sample symmetry, these are only three, or seven coefficients out of a total of 185. It is then possible to obtain these few texture coefficients by a fixed angle method which can be applied non-destructively and "on-line" in a sheet production line. In contrast hereto, a complete texture analysis requires a sample to be cut from the sheet and to measure its texture "off-line" on a texture goniometer.

The principles of the fixed-angle texture analyzer of Figure 1 are shown in Figure 2. The incident X-ray beam hits the sheet from one side and on the other side several energy dispersive detectors are placed the positions of which define the sample directions $y_i = \{\alpha_i, \beta_i\}$, at which pole density values are being measured. Each detector measures a diffraction spectrum from which the integrated intensities I_{ij} of several diffraction peaks $(hkl)_j$ can be obtained, Figure 3. We further assume that the measured intensities can be calibrated with a random sample which yields the intensities I'_{ij} . The pole density $A(y_i, h_j)$ of the diffraction peak $(hkl)_j$ at the sample direction y_i is then given by

$$A(y_i, h_j) = \frac{I_{ij}}{I'_{ij}} = A_{ij}^{\text{exp}} \quad (5)$$

The A_{ij}^{exp} -values are the primary output values of the texture analyzer. It is then the task to calculate $C_{\lambda}^{\mu\nu}$ -values according to Eq. (4) up to the necessary degree $L = L^0$ (see e.g. Bunge and Wang, 1987). If the material has a texture according

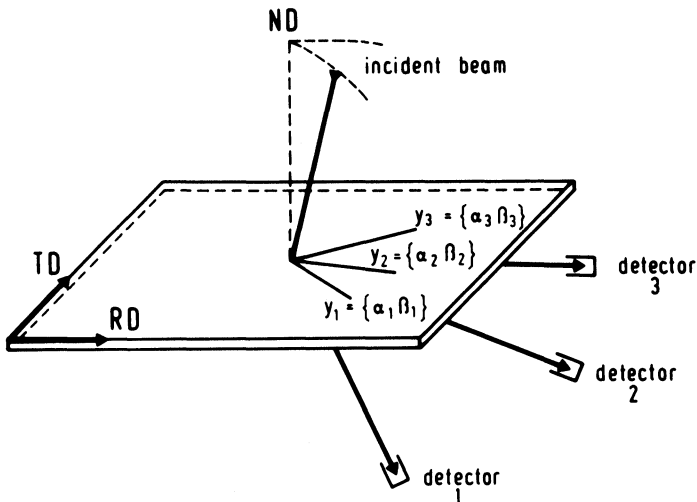


Figure 2 Incident beam, reflected beams and positions of pole figure points.

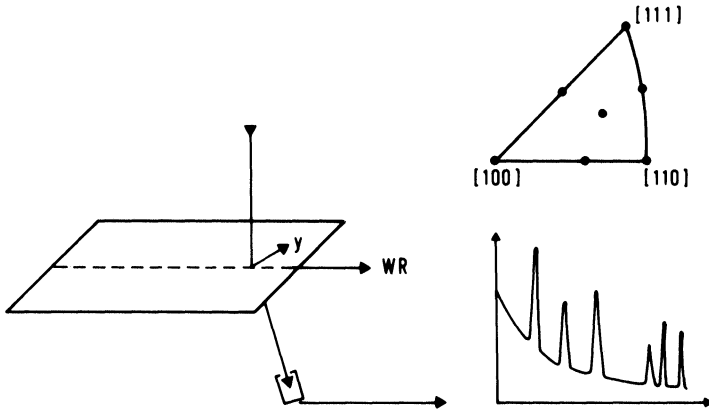


Figure 3 Energy dispersive measurement of several points of the inverse pole figure.

to Eq. (4) then theoretical A_{ij} values can be calculated

$$A_{ij}^{\text{theor}} = 1 + \sum_{\lambda=\lambda_0}^{L^0} \sum_{\mu=1}^{M(\lambda)} \sum_{\nu=1}^{N(\lambda)} \frac{4\pi}{2\lambda + 1} \cdot C_{\lambda}^{\mu\nu} \cdot \dot{K}_{\lambda}^{*\mu}(h_j) \cdot \dot{K}_{\lambda}^{\nu}(y_i) \tag{6}$$

where $\dot{K}_{\lambda}^{\mu}(h)$ and $\dot{K}_{\lambda}^{\nu}(y)$ are spherical harmonics with the crystal and sample symmetry respectively. These A_{ij} -values are of course unknown as long as the texture coefficients $C_{\lambda}^{\mu\nu}$ are unknown. Approximations to the texture coefficients $C_{\lambda}^{\mu\nu}$ can, however, be obtained by the condition

$$\sum_{i=1}^{i_{\max}} \sum_{j=1}^{j_{\max}} W_{ij} \cdot [A_{ij}^{\text{exp}} - A_{ij}^{\text{theor}}(L_0)]^2 = \min \tag{7}$$

with an appropriate value of L^0 . The quantities W_{ij} are weighting factors which may be chosen—in the simplest case—as $W_{ij} = 1$ or inversely proportional to the accuracy of the intensity I_{ij} . We put for abbreviation

$$\gamma_{\lambda}^{\mu'\nu'} = \sum_{i=1}^{i_{\max}} \sum_{j=1}^{j_{\max}} [A_{ij}^{\text{exp}} - 1] \cdot W_{ij} \cdot \dot{K}_{\lambda}^{*\mu'}(h_j) \cdot \dot{K}_{\lambda}^{\nu'}(y_i) \tag{8}$$

$$\alpha_{\lambda\lambda'}^{\mu\mu'\nu\nu'} = \sum_{i=1}^{i_{\max}} \sum_{j=1}^{j_{\max}} W_{ij} \cdot \frac{4\pi}{2\lambda + 1} \cdot \dot{K}_{\lambda}^{*\mu}(h_j) \cdot \dot{K}_{\lambda'}^{*\mu'}(h_j) \cdot \dot{K}_{\lambda}^{\nu}(y_i) \cdot \dot{K}_{\lambda'}^{\nu'}(y_i) \tag{9}$$

Then Eq. (7) leads to the condition

$$\sum_{\lambda=\lambda_0}^{L^0} \sum_{\mu=1}^{M(\lambda)} \sum_{\nu=1}^{N(\lambda)} L^0 C_{\lambda}^{\mu\nu} \cdot \alpha_{\lambda\lambda'}^{\mu\mu'\nu\nu'} = \gamma_{\lambda}^{\mu'\nu'} \tag{10}$$

where $L^0 C_{\lambda}^{\mu\nu}$ is an approximation of order L^0 to the unknown coefficients $C_{\lambda}^{\mu\nu}$ defined in Eq. (4) or (6). Equation (10) has the solution

$$L^0 C_{\lambda}^{\mu\nu} = \sum_{\lambda'=\lambda_0}^{L^0} \sum_{\mu'=1}^{M(\lambda')} \sum_{\nu'=1}^{N(\lambda')} \beta_{\lambda\lambda'}^{\mu\mu'\nu\nu'} \cdot \gamma_{\lambda'}^{\mu'\nu'} \tag{11}$$

where

$$\beta_{\lambda\lambda'}^{\mu\mu'\nu\nu'} = [\alpha_{\lambda\lambda'}^{\mu\mu'\nu\nu'}]^{-1} \tag{12}$$

is the inverse coefficient matrix to the matrix α in Eq. (10). Substituting finally $\gamma_{\lambda'}^{\mu'v'}$ in Eq. (11) by the expression Eq. (8) one obtains

$${}^{L^0}C_{\lambda}^{\mu\nu} = \sum_{i=1}^{i_{\max}} \sum_{j=1}^{j_{\max}} {}^{L^0}a_{\lambda}^{\mu\nu}(i, j) \cdot [A_{ij}^{\text{exp}} - 1] \quad (13)$$

with

$${}^{L^0}a_{\lambda}^{\mu\nu}(i, j) = W_{ij} \sum_{\lambda'=\lambda_0}^{L^0} \sum_{\mu'=1}^{M(\lambda')} \sum_{\nu'=1}^{N(\lambda')} \dot{K}_{\lambda'}^{\mu'}(h_j) \cdot \dot{K}_{\lambda'}^{\nu'}(y_i) \cdot \beta_{\lambda\lambda'}^{\mu'\nu'} \quad (14)$$

The coefficients ${}^{L^0}a_{\lambda}^{\mu\nu}$ are defined by Eq. (14, 12, 9). Hence, they depend only on the values h_j , y_i and L^0 . If these values once are fixed, the ${}^{L^0}a_{\lambda}^{\mu\nu}$ are purely mathematical constants which are independent of the experimental values A_{ij} .

Equation (6) is valid if the sample direction y_i is uniquely defined by the position of the i th detector. Practically this is only the case within the limits defined by the apertures used in the incident and reflected beam of the i th detector. Hence, all quantities depending on y_i have to be integrated over the aperture

$$\bar{I}_{ij} = \int I_i(y) \cdot \omega_i(y) dy \quad (15)$$

$$\bar{K}_{\lambda}^{\gamma}(y_i) = \int \dot{K}_{\lambda}^{\gamma}(y) \cdot \omega_i(y) dy \quad (16)$$

where $\omega_i(y)$ is the “transparency” function of the pole figure “window” defined by the apertures of the i th detector Figure 4. Then in Eq. (5) I_{ij} and I_{ij} are to be replaced by the values according to Eq. (15) and $\dot{K}_{\lambda}^{\gamma}(y_i)$ in Eqs. (6, 8, 9, 14) is to be replaced by the averaged value according to Eq. (16).

In Eq. (5) the calibration of the measurements with a random sample was assumed. It is, however, difficult to prepare a sample which is—on the one hand, exactly random within the required accuracy—and which is on the other hand

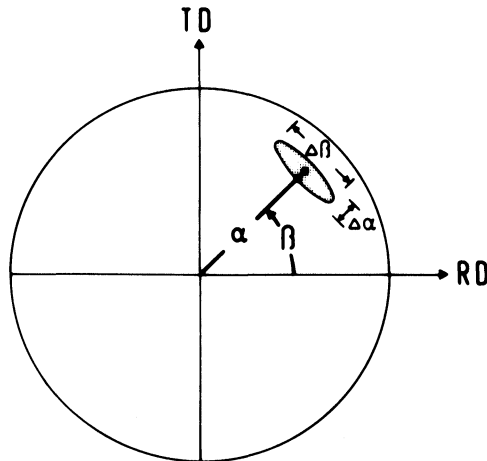


Figure 4 The divergencies of incident and reflected beam define a pole figure “window”.

Table 1 Texture coefficients $C_{\lambda}^{\mu\nu}$ up to $L^0 = 6$ of an annealed low-carbon steel compared with approximations of these coefficients calculated with various numbers of pole figure points and in two different approximations $L^0 = 6$ and $L^0 = 4$ (one pole figure means 343 points).

$C_{\lambda}^{\mu\nu}$	True coefficient	Analysis from 3 pole figures up to $l_{max} = 22$	Analysis from 1 pole figure up to $l_{max} = 10$	Analysis from 20 points up to $l_{max} = 6$	Analysis from 20 points up to $l_{max} = 4$
C_4^{10}	-1.602	-1.596	-1.606	-1.717	-1.818
C_4^{12}	-0.126	-0.125	-0.121	-0.267	-0.184
C_4^{14}	0.591	0.588	0.586	0.603	0.572
C_6^{10}	-2.460	-2.435	-2.435	-1.865	
C_6^{12}	0.983	0.973	0.972	1.244	
C_6^{14}	-0.270	-0.267	-0.266	-0.662	
C_6^{16}	0.321	0.317	0.316	0.337	

also comparable with the test sample in all other respects (relative density, line broadening and others). In this case any other sample with a known texture can also be used for calibration. Similar to Eq. (5) the intensities measured in the calibration sample are

$$I_{ij}^{cal} = I_{ij} \cdot A_{ij}^{cal}(L) \tag{17}$$

with $A_{ij}^{cal}(L)$ according to Eq. (6) with the known texture coefficients of the calibration sample and a sufficiently high degree L . Equation (5) can then be transformed to

$$A_{ij}^{exp} = \frac{I_{ij}}{I_{ij}^{cal}} \cdot A_{ij}^{cal}(L) \tag{18}$$

If a *nearly random sample* is available then the factors $A_{ij}^{cal}(L)$ in Eq. (18) are correction factors near to one. When the coefficients $L^0 a_{\lambda}^{\mu\nu}(i, j)$ have been calculated then Eq. (13) provides an approximation $L^0 C_{\lambda}^{\mu\nu}$ to the correct coefficients $C_{\lambda}^{\mu\nu}$ which can be proven if the theoretical values $C_{\lambda}^{\mu\nu}$ are known. This test can be achieved purely “mathematical” without taking recourse to real measurements. For this purpose the A_{ij} in Eq. (13) can be replaced with A_{ij} -values calculated by Eq. 6 with a sufficiently high degree L . The A_{ij} are then ideal “experimental” values belonging to an exactly known texture with the coefficients $C_{\lambda}^{\mu\nu}$. These A_{ij} -values have furthermore the advantage that they are free of experimental errors. Hence, they are very well suited to test the proposed mathematical procedure. Tests of this type were carried out for several assumed experimental conditions some examples of which are given in Table 1. It is seen that, with a reasonable choice of the experimental conditions, the degree of approximation is quite satisfactory.

References

- Bunge, H. J. (1982). *Texture Analysis in Materials Science*. Butterworth Publ. London.
- Bunge, H. J. (1987). Three Dimensional Texture Analysis. *Intern. Mat. Rev.*, **32**, 265–291.
- Bunge, H. J. (1989). Texture and Magnetic Properties. *Textures and Microstructures* **11**, 75–91.
- Bunge, H. J. and Wang, F. Computational Problems in Low Resolution Texture Analysis. In: *Theoretical Methods of Texture Analysis*. Ed. H. J. Bunge DGM Informationsgesellschaft, Oberursel 1987 p. 163–172.
- Kopineck, H. J. On-Line Texture Measurement in a Production Line. In: *Experimental Techniques of Texture Analysis*. Ed. H. J. Bunge DGM Informationsgesellschaft, Oberursel 1986 p. 171–190.
- Kopineck, H. J. and Otten, H. (1987). Texture Analyzer for On-Line r_m -Value Estimation. *Textures and Microstructures* **7**, 97–114.
- Kopineck, H. J. and Bunge, H. J. (1988). A Fixed Angle Texture Analyzer For Texture Inspection and Property Control in Sheet Production Lines. In: *Directional Properties of Materials*. Ed. H. J. Bunge, DGM Informationsgesellschaft, Oberursel pp. 251–262.